An RF BIST Architecture for Output Stages of Multistandard Radios

Emanuel Dogaru, Filipe Vinci dos Santos, William Rebernak

An RF BIST Architecture for Output Stages of Multistandard Radios

Emanuel Dogaru*†, Filipe Vinci dos Santos* and William Rebernak†
*Thales Chair on Advanced Analog Design, SUPELEC
Gif-sur-Yvette, France
Email: filipe.vinci@supelec.fr
†THALES Communications & Security
Gennevilliers, France

***Abstract*—Software defined radios (SDR) platforms are increasingly complex systems which combine great flexibility and high performance. These two characteristics, together with highly integrated architectures make production test a challenging task. In this paper, we introduce an Radio Frequency (RF) Built-in Self-Test (BIST) strategy based on Periodically Nonuniform Sampling of the signal at the output stages of multistandard radios. We leverage the I/Q ADC channels and the DSP resources to extract the bandpass waveform at the output of the power amplifier (PA). Analytical expressions and simulations show that our time-interleaved conversion scheme is sensitive to time-skew. We show a time-skew estimation technique that allows us to surmount this obstacle. Simulation results show that we can effectively reconstruct the bandpass signal of the output stage using this architecture, opening the way for a complete RF BIST strategy for multistandard radios. Future developments will be focused on an efficient mapping to hardware of our new time-skew estimation for TIADC bandpass conversion.**

***Keywords*—BIST, Periodically nonuniform sampling, software radios, SDR, mixed-signal test, undersampling**

I. Introduction

The unabated improvement in speed and integration density of integrated circuits (IC) has made possible the Software Defined Radio concept proposed by Mitola [1]. An SDR is a Radio in which some (or all) of the physical layer functions are programmable. These architectures are well suited to the requirements of the defense sector (secure military communication terminals). The outstanding flexibility and performance of these radios result from careful trade-offs among advanced analog/RF circuitry, high-speed reconfigurable digital hardware and sophisticated real-time software. However, the inherent adaptability of these multistandard platforms hinders the testability of the finished units. Established mixed-signal and RF test strategy are either too time-consuming (thus costly) or can't ensure compliance with several modulations standards, including those yet to appear. Unlike conventional transmitters, SDR platforms must satisfy strict requirements under a wide variety of operating modes. New test strategies must be invented, able to cover thoroughly and efficiently all key specifications of the radio unit.

Over the past few years, analog and mixed-signal test and testability has been a subject of intense research. Traditional production testing of transceivers relies on specialized machines, known as Automatic Test Equipment (ATE) units, [2], [3]. ATEs are fast, accurate and reconfigurable, but also very expensive and hard to master. These shortcomings gave rise to continuing research efforts for cost effective alternatives.

One such alternative, borrowed from digital testing research, is the idea of introducing Built-In Self-Test (BIST) techniques to eliminate or reduce the need for external instrumentation. Analog and mixed-signal (AMS) BIST techniques generally entail additional circuitry and reuse of resources already present (DSP, converters, memory).

Several AMS BIST techniques targeting specifically RF transceivers (RF BIST) have been proposed. RF BIST strategies generally try to avoid to route RF signals from or to external equipment. The loopback approach is one of the most cited RF BIST technique (see [4], [5], [6], [7], [8]). In a nutshell, RF loopback consists in using the transmitting part (Tx) to excite some parts or all of the receiver (Rx). The key point is to add components that allow the reconfiguration of the on-board (or on-chip) resources to carry out some type of characterization.

Loopback BIST is an attractive proposition, although it has two major drawbacks. The first one is fault masking, a situation where a (non-catastrophic) failure of the Tx is covered up by an exceptionally good Rx, or the inverse. A marginal product could then go undetected (test escapes). The second drawback of BIST loopback is that it is not applicable directly to all transceivers architectures (e.g. [9]). In spite of its shortcomings, loopback BIST has been often implemented and reported as effective: [4], [5], [10], [6], [8], [7]. The large number of publications shows the continuing interest in the topic.

From the point of view of SDR platforms, a common shortcoming of all RF BIST proposals is that they are tied to a specific operating condition (frequency, modulation, standard, etc.), and cannot adapt to the wide range of operating modes of tactical radio units. In this paper we introduce a loopback BIST technique that overcomes this limitation.

The aim of our work is to reduce post-manufacture test cost of SDR transceivers by leveraging the reconfigurability of the platform. We are exploring the use of nonuniform sampling (undersampling) to carry out bandpass AD conversion of the PA signal, using I/Q channel ADCs as a single time-interleaved ADCs (see Fig. 1). Our initial efforts are focused to the

This project is supported by grants from ANRT and Thales Communications and Security

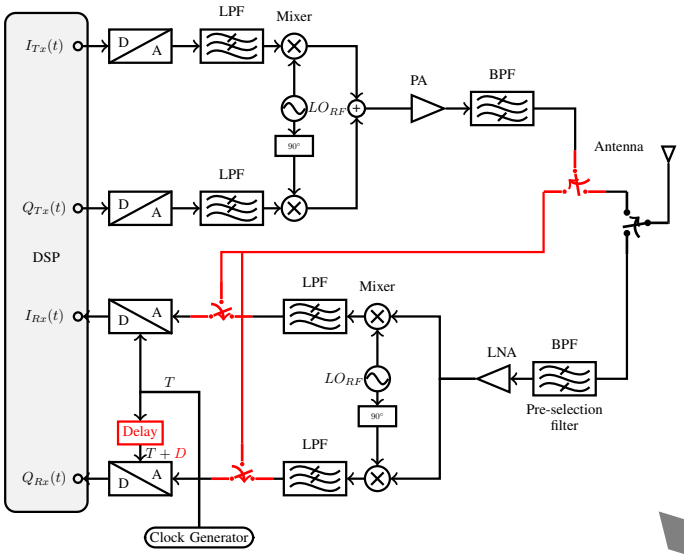

Fig. 1. Architecture of a homodyne transceiver. The red blocks are the modifications required by the RF BIST technique we propose.

characterization of the transmitter (Tx) chain with respect to compliance to the spectral mask. The bandpass measurements of the output stage waveforms using nonuniform sampling allow us to surmount the most vexing post-manufacture test issue for tactical radio units. Our approach is scalable across a wide range of complex specifications without incurring additional hardware or performance cost. As presented in this paper, the technique we propose is more suitable for offline utilization.

This paper gives a detailed description of our bandpass nonuniform sampling architecture. First, we describe the mathematical basis for the technique, and give theoretical results suggesting its feasibility. We show then that the implementation requirements can be met with reasonable margin without affecting the robustness of signal reconstruction. The most critical requirement is shown to be the time-skew between channels. The feasibility of using time-skew measurement techniques commonly applied to Time-Interleaved ADCs (TIADCs) is analyzed, and experimentally demonstrated with a typical configuration. The results obtained in simulations are promising, pushing us to advance to a hardware implementation.

To confirm the results of our mathematical analysis we built a behavioral model of a homodyne transmitter and ran extensive simulations. We choose to use `Matlab`, and later `SystemC-AMS`, in order to obtain highly accurate results while handling disparate time constants, within reasonable simulation times. Our simulations show that the time-skew is indeed critical to our approach, and that it can be estimated to the required level by well known-techniques.

The remainder of this paper is organized as follows. Section II introduces the mathematical theory behind the periodical nonuniform sampling technique and motivates our choice. Section III describes a practical realization of the nonuniform sampler that uses a modified time-interleaved ADC, and discusses the obstacles found. Section IV provides a time-skew detection technique that improves BP-TIADC performances.

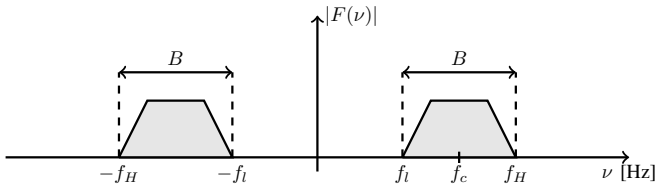

Fig. 2. Bandpass Signal

Section V shows the results obtained in simulation. Finally, our conclusions and future developments are given in Section VI.

II. Theoretical Background

It is well known that a continuous time signal $f(t)$ with Fourier transform $F(\nu)$, limited to a non-zero frequency range $|\nu| < B$ can be reconstructed from its samples $f(nT/2)$, where $T = 1/B$. This technique is well known as Nyquist [illegible]. It has also been demonstrated in [11], [12] that if $F(\nu)$ is [illegible] to a frequency range $f_l < |\nu| < f_l + B$ (see Fig. 2), then $f(t)$ can also be reconstructed from a set of uniformly spaced samples $f(nT/2)$, as long as the ratio f_l/B [illegible] positive ratios integer. This sampling scheme is called Periodically Bandpass Sampling of First Order (PBS) or Uniform Bandpass Sampling. If the previous requirements [illegible] band locations are not met, Kohlenberg [12] showed that $f(t)$ can still be reconstructed from two sets of uniform samples $f(nT)$ and $f(nT+D)$. This sampling scheme is called Periodically Nonuniform Bandpass Sampling of Second Order (PNBS) and it will be presented in details in a further section.

In this section we present a succinct comparison between the two bandpass sampling techniques. We then show the advantages of using nonuniform sampling over uniform sampling for narrowband signals located at high frequency in the context of SDR testing. Afterward, we will examine some concerns and potential problems arising from practical implementations of a nonuniform sampler.

A. Periodic Bandpass Sampling

The advantage of bandpass sampling over Nyquist baseband sampling for RF systems is clear: the sampling frequency needed and the subsequent processing rate are proportional to the information bandwidth, rather than to the center (carrier) frequency.

The periodically uniform sampling technique is commonly used in bandpass sampling receivers, [13], [14]. The frequency domain view of ideal PBS is illustrated in Fig. 3. The red zone of spectrum represents the desired bandpass signal. The ideal sampling operation shown creates replicas of the original spectrum in each Nyquist zone. A bandpass filter (BPF) is required, otherwise unwanted signals outside the desired bandpass range will also appear at the 1st Nyquist zone (baseband).

The superposition of spectra due to frequency folding (aliasing) is a concern for the choice of sampling frequency f_s. In effect, the relationship among f_s, signal bandwidth B, and upper range limit f_H is constrained if spectral superposition must be avoided. The feasible combination are depicted graphically in Fig. 4a (see [15]), where f_s and f_H are normalized w.r.t. signal bandwidth B. The white regions

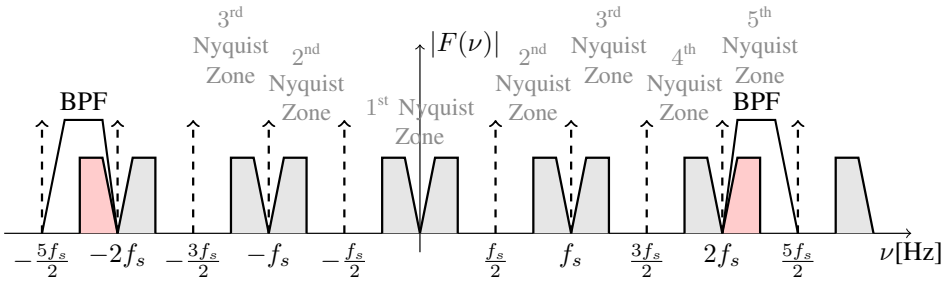

Fig. 3. Frequency spectrum illustration of standard bandpass sampling

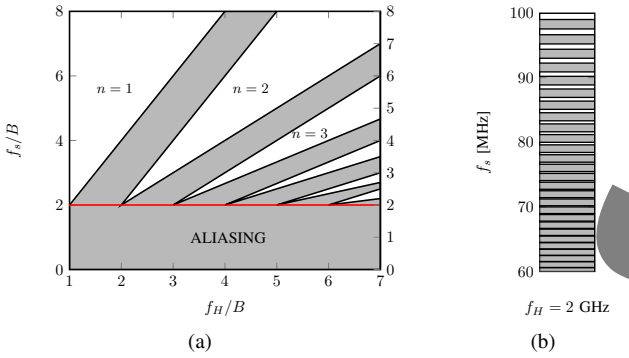

Fig. 4. The constraints on the sampling rate f_s for PBS as presented in [15]: (a) the general case and (b) a particular case where $f_H = 2.03$ GHz and $B = 30$ MHz.

represent the situations where the bandpass sampling will not result in aliasing. The gray regions represents conditions where alias is occurring. One readily observes that the minimum ideal sampling rate is $f_s = 2B$, as expected, but there is little margins for imperfections in the actual implementation. The sensitivity increases as f_H/B increases. Therefore, practical implementations of uniform bandpass sampling must sample faster than the theoretical minimum rate and even, then, faster rates will avoid aliasing, if the signal band is not well positioned.

Let's consider as numerical example a $B = 30$ MHz bandpass signal located at $f_l = 2$ GHz. In this example the acceptable sample rates are described by the gray areas in Fig. 4b. If a sampling rate around the ideal minimum $2B$ is needed, the subsampling clock should have a precision of few KHz in order to avoid aliasing. The most obvious solution to relax these constraints is to use guards bands (which is equivalent to sampling at nonminimum rates, see [15]). Even so, in the example from Fig. 4b, the sampling around $f_s = 90$ MHz (larger than $2B$) would still require sampling precision of few hundreds of KHz.

Finally, if the center frequency of the signal changes, the acceptable samples rates also change and need to be recalculated.

To sum up, uniform bandpass sampling is effective, but [illegible] implement without incurring aliasing problems as the ratio $f_H/$ [illegible] rises.

B. Periodically Nonuniform Bandpass Sampling (PNBS)

The discussions above suggest that the PBS technique is not well suited for test of software radios due to the lake of flexibility. Indeed, one of the most important characteristics of a software radio is its flexibility. That means that it is capable to operate over a wide range of operating parameters (frequency, data rate, modulation type, etc.). A well designed test strategy should be able to cover all of these configurations, with minimum of effort and extra circuitry. This it is not the case where PBS is employed.

An alternative solution to the PBS is the PNBS technique. PNBS allows the reconstruction of bandpass signals from two sets of uniformly spaced samples, at the theoretical minimal rate and independent of the band locations (the straight red line in Fig. 4). This technique allows overcoming the limitations of the PBS and offers a higher level of flexibility.

Bandpass signal reconstruction from nonuniform samples was introduced in [12] with further results given in [11], [15]. Kohlenberg [12] showed that a bandpass signal $f(t)$ (Fig. 2) can be reconstructed from two sets of uniform samples, $f(nT)$ and $f(nT + D)$ using the exact interpolation relation:

$$f(t) = \sum_{n=-\infty}^{+\infty} [f(nT)s(t - nT) + f(nT + D)s(nT + D - t)] \tag{1}$$

where $T = 1/B$, D represents the phase delay and:

$$s(t) = s_0(t) + s_1(t) \tag{2a}$$

$$s_0(t) = \frac{\cos[2\pi(kB - f_l)t - k\pi BD] - \cos[2\pi f_l t - k\pi BD]}{2\pi Bt \sin k\pi BD} \tag{2b}$$

$$s_1(t) = \frac{\cos[2\pi(f_l + B)t - (k+1)\pi BD] - \cos[2\pi(kB - f_l)t - (k+1)\pi BD]}{2\pi Bt \sin(k+1)\pi BD} \tag{2c}$$

$$k = \left\lceil \frac{2f_l}{B} \right\rceil, \text{ where } \lceil * \rceil \text{ is the ceiling operator} \tag{2d}$$

Proofs for equations (1), (2) and (3) and further discussions regarding the stability of reconstruction can be found in [12], [11]. In this paper our concern is the practical realization of a nonuniform sampler within a typical SDR platform. In the following we present some considerations regarding the choice of the delay D, that directly affect the architecture of the nonuniform sampler we propose.

1) Choice of D: The relation (1) is valid provided that D meets the following constraints:

$$D \neq nT/k \tag{3a}$$
$$D \neq nT/(k+1), \forall n \in \mathbb{N} \tag{3b}$$

If D assumes values which violate the conditions (3) then the reconstruction filter becomes unstable. If $k = \frac{2f_l}{B}$, the first term of the reconstruction filter $s_0(t)$ is 0 and the condition (3a) no longer applies.

The nonuniform sampling of $f(t)$ can be done by two identical ADCs, both running at the sample rate, f_s, but triggered with a constant time delay D. Conceptually sp ing, it is clear that the value assumed by the delay D critical for the accuracy and computational cost of the signal reconstruction from the nonuniform sampled values. One can observe that if D approaches the right-hand values given in (3), the coefficients of the reconstruction filter rise progressive toward infinity. Unduly large values complicate the practi realization, since more terms will have significant values a will have to be more precisely computed. The authors in [showed that the optimal values of D w.r.t. the magnitude o the coefficients filter in (1) are $D = \pm 1/(4f_c)$.

2) Reconstruction Robustness: There are other pra ical concerns with respect to the values of D (1). Our to use slow time-interleaved ADCs to obtain nonuniform spaced samples of $f(t)$. In order to apply the relation (1), D must be known. Enforcing an accurate valu tricky, since the accuracy required is relate o the value the carrier frequency. Let say that instead knowing the real value of D, only an estimate $\hat{D} = D + \Delta D$ s available. It has been shown in [15] that the relative dif ence between the reconstructed spectrum $\hat{F}(\nu)$ and the a pectrum $F(\nu)$ can be approximated as:

$$\Delta F = \left| \frac{\hat{F}(\nu) - F(\nu)}{F(\nu)} \right| \approx \pi B(k+1)\Delta D \tag{4}$$

Equation (4) shows that, as the rapport between the center frequency and the signal bandwidth increases, the acceptable values for ΔD become very small. Moreover the precision of reconstruction depends also on the high frequency f_c, and not only on the signal bandwidth B, as it would be desirable. This means that for higher carrier frequency, the estimation of D should be more accurate.

For example, for a bandpass signal at $f_c = 1$ GHz to be recovered from the samples of two ADCs running at $f_s = B = 80$ MHz with a precision of $\Delta F = 1\%$, ΔD must respect:

$$\Delta D \leq \frac{1}{25} \frac{0.01}{\pi 80 \cdot 10^6} \approx 2 \text{ ps} \tag{5}$$

The result from (5) is important because it proves that a robust bandpass reconstruction with PNBS is feasible. Indeed, there are several hardware implementations reported in literature (see [16], [17]) that can estimate and correct the time-skew between two ADCs with a granularity of few ps. Finally, equation (4) and the example from (5) establish that the most critical point while reconstructing a bandpass signal using nonuniform sampling is the accurate knowledge of D.

3) Remarks: The main objective of this paper is to propose a nonuniform bandpass sampling architecture and a delay identification technique that will overcome the obstacles previously discussed. Using the SDR capabilities and the bandpass nonuniform sampler, our final purpose is to reconstruct and to observe the spectrum at the output of the Tx.

Before to propose a practical implementation of nonuniform sampler it is important to discuss its limitations:

- Noise Considerations. Compared to a classic analog receiver that uses mixers to translate the signal to a bandpass sampling technique degrades the Signal-to-Noise Ratio of the original signal. Even if a bandpass filter is used, the thermal noise is still aliased to the band of interest [15], [14]. For our purpose, limitation is not a concern because we are more interested to characterize the Tx at higher signals level.
- Phase Noise. It is well known that the phase noise the sampling clock limits the performances of the ndpass sampling technique [13]. Anyway, in [18] authors showed that the clock jitter requirement r a bandpass sampling receiver are similar to the requirements for the local oscillator (LO) in a mixing receiver.
- Sample and Hold (S/H) circuits. The analog input bandwidth of the S/H circuits must cover all the RF signals we want to monitor. If it's not the case with the S/H integrated in the Rx ADCs, we may want to consider introducing two S/H circuits before the ADCs in Fig. 1.

III. Proposed Architecture

The theoretical results presented in the previous section allowed us to derive the general requirements on a nonuniform sampler designed to reconstruct a high-frequency bandpass signal. The architecture we are proposing is similar to a two-channel time-interleaved ADC (TIADC). Both architectures share the same limitations. This is why we start this section by giving a short overview of the TIADCs and their main problems.

A. Time-Interleaved Analog-to-Digital Converter

Fig. 5 shows a simplified block diagram of a two channels time-interleaved ADC. It consists of two ADCs operating in parallel at half of the overall sampling rate $f_s = 1/T$. Theoretically, this interleaved structure would allow to multiply the overall sample rate achieved by each channel ADC without degrading other properties (resolution, distortion, etc.). This is not the case. The overall conversion properties worsen due to the unavoidable mismatches between different channels of a manufactured chip. The most important are offset error, gain

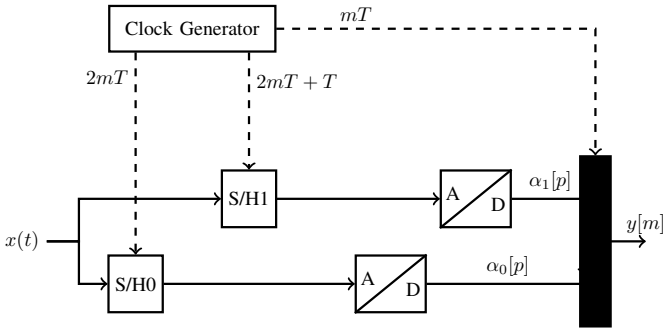

Fig. 5. Block diagram of the two channels time-interleaved ADC architecture

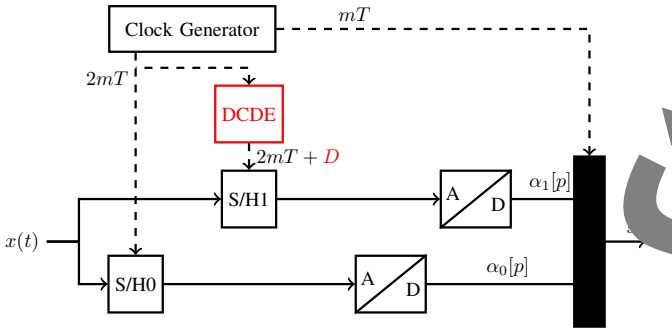

Fig. 6. Block diagram of the proposed BP-TIADC architecture. The difference between this architecture and the one presented in Fig. 5 is the Digitally Controlled Delay Element (DCDE) that will introduce a controlled delay D

error, and time-skew. The time-skew appears when the delays between the different ADCs are not equal. The sampling period is not constant, which will result in distortion of the reconstructed signal.

These limitations were recognized from the beginning and channel mismatch calibration strategies have been continuously introduced. The offset and the gain error calibrations are relatively simple to implement (see [19], [20]), and they will not be discussed further here. Time-skew calibration, on the other hand, is a more challenging task. It requires estimation and correction of sample time error across channels. Time-skew calibration can be performed separately (offline, [20]) or concurrently (online) with the normal use of the TIADC.

B. Bandpass TIADC Architecture

In this section we will describe a candidate architecture for a bandpass TIADC using the periodic nonuniform sampling. It is shown that existing estimation schemes can be adapted to nonuniform sampling BP-TIADC, helping their performances.

The nonuniform BP-TIADC architecture is shown in Fig. 6. It is only slightly different from the standard TIADC shown in Fig. 5. The key block is the Digitally Controlled Delay Element (DCDE) shown in red. The function of the DCDE is to adjust the delay D such that it meets the constraints of Equation (3), as explained in Section II-B.

At this point, it is important to recall our objective: the design of a nonuniform bandpass sampler for the output

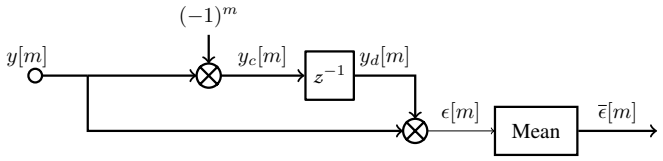

Fig. 7. Block diagram of the time-skew detector as proposed in [17]. $y[m]$ is the output of the BP-TIADC from Fig. 6

stage of an SDR. The receiver side of an SDR platform integrates two powerful ADCs that are not used usually during transmission. Therefore, we propose to reuse these two ADCs for Tx test purposes. The required modifications are presented in red in Fig. 1. As result, the additional hardware required is reduced at minimum and the effort of calculus is shifted toward the software/digital domain.

As expected, the mismatches described in the previous section (offset error, gain error and time-skew) also affect the BP-TIADC performances but, as we will see, it is easier to minimize these effects. One should note that the time-skew calibration in standard TIADC architectures is a more difficult task since one must estimate the delay across channels and then suppress it. The critical path for the calibration is this correction, which typically hits the ultimate limits of the underlying technology. This is not the case for the BP-TIADC with nonuniform sampling, where a null (or exact) adjustment of time-skew is not necessarily. The challenge is how to estimate it accurately. The estimation problem will be discussed in the following section.

IV. Time-Skew Detection Technique

In this section we discuss a time-skew identification technique proposed by [16], [17]. The choice is motivated by the high performances achieved by this technique, while keeping a simple practical implementation.

Let us consider the architecture in Fig. 6. The system response to the sinusoid input $x(t) = \cos(\omega_0 t), 0 < \omega_0 < \omega_s/2$ is:

$$y[m] = \cos(\omega_0 t)|_{t=mT+\frac{d}{2}-(-1)^m\frac{d}{2}} \tag{6}$$

where $d = D - T$ and $\omega_s = 2\pi f_s = 2\pi/T$. After several manipulations:

$$y[m] = \cos\left[\frac{\omega_0 d}{2}\right]\cos\left[\omega_0 mT + \frac{\omega_0 d}{2}\right] - \sin\left[\frac{\omega_0 d}{2}\right]\sin\left[(-\omega_0 + \frac{\omega_s}{2})mT - \frac{\omega_0 d}{2}\right] \tag{7}$$

Using the previous observations, the authors in [17] propose the architecture depicted in Fig. 7 as a technique to identify the delay between the two ADCs. In the following, we will present succinctly the technique. The output of the BP-TIADC, $y[m]$ is chopped to produce $y_c[m]$ and then is passed through a delay filter to produce $y_d[n]$. $y[m]$ and $y_d[m]$ are

then multiplied. The chopped signal $y_c[m]$ can be written as:

$$\begin{aligned} y_c[m] &= (-1)^m y[m] \\ &= a\cos\left[\left(\frac{\omega_s}{2}-\omega_0\right)mT-\frac{\omega_0 d}{2}\right] \\ &\quad +b\sin\left[\omega_0 mT+\frac{\omega_0 d}{2}\right] \end{aligned} \tag{8}$$

where $a=\cos(\omega_0 d/2)$ and $b=\sin(\omega_0 d/2)$

The chopped signal goes through a delay filter, z^{-1} to produce :

$$\begin{aligned} y_d[m] &= a\cos\left[\left(\frac{\omega_s}{2}-\omega_0\right)(m-1)T-\frac{\omega_0 d}{2}\right] \\ &\quad +b\sin\left[\omega_0(m-1)T+\frac{\omega_0 d}{2}\right] \end{aligned} \tag{9}$$

Then $y[m]$ and $y_d[m]$ are multiplied, the product having a dc that is equal to:

$$\begin{aligned} \bar{\epsilon} &= \overline{y_d \cdot y} = -ab\sin(\omega_0 T) \\ &= -\cos\left(\frac{\omega_0 d}{2}\right)\sin\left(\frac{\omega_0 d}{2}\right)\sin(\omega_0 T) \end{aligned} \tag{10}$$

If we replace d with $D-T$, equation (10) becomes:

$$\bar{\epsilon} = -\sin(\omega_0 D-\omega_0 T)\sin(\omega_0 T) \tag{11}$$

If $|\omega_0 D| << 1$, (11) can be simplified to:

$$\bar{\epsilon} \approx -\frac{\omega_0 D}{4}\sin(2\omega_0 T)+\frac{\sin^2(\omega_0 T)}{2} \tag{12}$$

Equation (12) proves that the block presented in Fig. 7 outputs a value that allows the identification of the time-skew D. While having a simple practical implementation, this technique has some limitations. First of all, the input signal has to be bandlimited to less then $\omega_s/2$ and should not have a frequency component at $\omega_s/4$ (for a proof see [17], [16]). It follows from (11) that $\bar{\epsilon}$ peaks when the input frequency, ω_0 is near $\omega_s/4$ and decreases at higher input frequencies. The sensitivity of time-skew detection will follow the same trend.

V. Simulation Results

In order to validate the theoretical framework presented in this paper, the behavioral model of a homodyne transmitter is considered. Because of its flexibility, high level of integrability and good performances, the homodyne transmitter became nowadays the first choice while designing a RF system [22]. The block diagram of a homodyne transmitter is depicted in Fig. 1.

The periodically nonuniform technique, on which the entire framework is based, requires a explicitly simulation of each carrier cycle. However, to keep the computational effort reasonable, the simulations presented in this paper are based on behavioral-passband models [23]. Because of the mixed nature of the studied architecture, simulations are carried out in `Matlab`.

The homodyne transmitter is driven by 10 MHz QPSK symbols shaped by a square root raised cosine filter with a roll-off factor of $\alpha = 0.5$. The signal is then translated at the frequency $f_c = 1$ GHz.

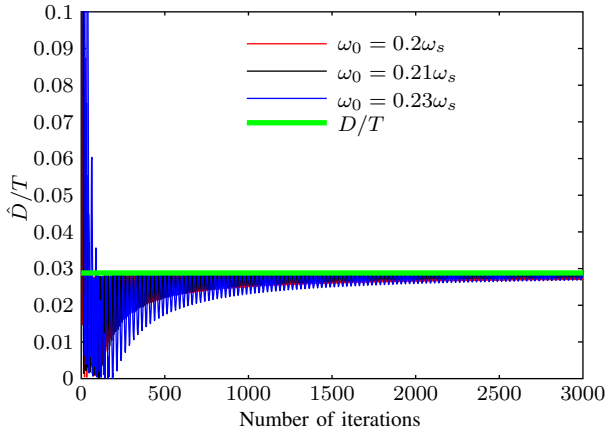

Fig. 8. Time-skew estimation over time. Figure shows the values $\hat{D}/T$ for several values of ω_0

RP-TIA[illegible] architecture is composed by two 10 bits ADCs, [illegible] operating at $B = 80$ MHz $\Longrightarrow f_s = 2B = 160$ MHz and $T = 1/f_s$. We consider that there are no gain or offset mismatches between the two ADCs. For these values of f_c [illegible] the first for forbidden value for D is $1/B(k+1) = 480$ ps. Therefore, delay D is fixed to 180 ps ($D/T = 0.028$). The clock generator that drives the sample-and-hold circuit has [illegible]um time-skew noise of amplitude 3 ps.

To evaluate the performances of the digital time-skew detection technique presented in Section IV, several simulations [illegible] different values of $\omega_0 \in [0.2\omega_s, 0.24\omega_s]$ were carried out. Fig. 8 shows the estimation $\hat{D}/T$ over time as obtained from the output $\bar{\epsilon}$ of the time-skew detector presented in Fig. 7 and from (12) for several values of ω_0. It can be observed that the estimations $\hat{D}/T$ converge to ideal value of D/T every time.

From now on, for each ω_0 only the last estimation $\hat{D}$ will be kept and analyzed. Table I presents a more detailed analysis of the results. Three metrics of interest are calculated. The second column represents the absolute difference between the value of D and the estimation $\hat{D}$, while the third column shows shows the relative differences between the same variables.

Because the estimated value of D will be used by a periodically nonuniform sampling technique, a much more interesting metric is the relative error between the real signal and the reconstructed values:

$$\Delta\varepsilon\left(f_{\hat{D}}^{2T}(\mathbf{t})\right) = \frac{\left\|f(\mathbf{t})-f_{\hat{D}}^{2T}(\mathbf{t})\right\|}{\|f(\mathbf{t})\|} \tag{13}$$

where $f_D^{2T}(t)$ is the practical reconstruction function of $f(t)$ from the samples $f(2nT)$ and $f(2nT+D)$:

$$\begin{aligned} f_D^{2T}(t) = \sum_{n=-n_w/2}^{+n_w/2} &[f(2nT)s(t-2nT) \\ &+f(2nT+D)s(2nT+D-t)] \end{aligned} \tag{14}$$

and $\mathbf{t} = \{t_i, i = \overline{1,N}\}$ is a vector of N time values.

$\Delta\varepsilon\left(f_{\hat{D}}^{2T}(\mathbf{t})\right)$ is a measure of how close from $f(\mathbf{t})$ are the reconstruction $f_{\hat{D}}^{2T}(\mathbf{t})$. In order to calculate this metric, we choose $N = 1000$ random time values from the interval

TABLE I. TIME-SKEW ESTIMATION ANALYSIS

	$\lvert\hat{D}-D\rvert$	$\lvert 1-\hat{D}/D\rvert$	$\Delta\varepsilon\left(f_{\hat{D}}^{2T}(\mathbf{t})\right)$
$\hat{D}=D$	0	0	1%
$\omega_0=0.2\omega_s$	5 ps	2.8%	3.5%
$\omega_0=0.21\omega_s$	1.1 ps	0.6%	1.2%
$\omega_0=0.23\omega_s$	0.3 ps	0.1%	1%

$[476\text{ ns}, 1700\text{ ns}]$, we calculate $f_{\hat{D}}^{2T}(\mathbf{t})$ using (14) and then the metric $\Delta\varepsilon\left(f_{\hat{D}}^{2T}(\mathbf{t})\right)$ is calculated using (13). This metric is presented in the fourth column of Table I.

As proved in theory, the digital time-skew detection technique manages to offer a good estimation of D. Moreover, the estimation, $\hat{D}$ for the last two rows in Table I respect the requirements imposed by (4) and (5). It can be seen from the Table I that the sensitivity of time-skew detection increases as ω_0 approaches $0.25\omega_s$. Finally, one can note that this detection technique is sensitive to the value of ω_0, which is a drawback.

VI. CONCLUSIONS AND FUTURE WORKS

In this paper, we introduced an RF BIST strategy based on Periodically Nonuniform Sampling of the signal at the output stages of multistandard radios. We leverage the I ADC channels and the DSP resources to extract the bandp waveform at the output of the power amplifier (PA). Analyti expressions and simulations show that our time-interleave conversion scheme is sensitive to time-skew. We presented a time-skew estimation technique that allows us to sur unt this obstacle. Simulation results show that we can effec ely reconstruct the bandpass signal of the output stage us architecture, opening the way for a complete RF BIST strategy for multistandard radios.

Future developments will be focused on efficient ma ping to hardware of our new time-skew esti tion for TIADC bandpass conversion.rm ADC.

REFERENCES

[1] I. Mitola, J., "Software radios: Survey, critical evaluation a directions," *IEEE Trans. Aerosp. Electron. Syst.*, vol. 8, no. 4, pp. 25 36, 1993.

[2] R. Wolf, M. Slamani, J. Ferrario, and J. Bhagat, *Advances in Electronic Testing: Challenges and Methodologies*. Netherlands: Springer, 2006, ch. 10 - RF Testing.

[3] P. Cruz, N. Carvalho, and K. Remley, "Designing and testing software-defined radios," *IEEE Microw. Mag.*, vol. 11, no. 4, pp. 83–94, 2010.

[4] M. Onabajo, J. Silva-Martinez, F. Fernandez, and E. Sanchez-Sinencio, "An on-chip loopback block for RF transceiver built-in test," *IEEE Trans. Circuits Syst. II*, vol. 56, no. 6, pp. 444–448, 2009.

[5] M. Negreiros, L. Carro, and A. A. Susin, "Reducing test time using an enhanced RF loopback," *J. Electron. Testing*, vol. 23, no. 6, pp. 613–623, 2007.

[6] J. Dabrowski and J. Bayon, "Mixed loopback BIST for RF digital transceivers," in *Proc. IEEE Defect and Fault Tolerance in VLSI Systems (DFT 2004)*, Oct. 2004, pp. 220 – 228.

[7] A. Nassery and S. Ozev, "An analytical technique for characterization of transceiver IQ imbalances in the loop-back mode," in *Design, Automation Test in Europe (DATE), Conf. Exhibition*, 2012, pp. 1084–1089.

[8] A. Haldes, S. Bhattacharya, G. Srinivasan, and A. Chaterjee, "A system-level alternate test approach for specification test of RF transceivers in loopback mode," in *Proc. Int. Conf. on VLSI Design (VLSID'05)*, 2005, pp. 132–137.

[9] J. Dabrowski and R. Ramzan, "Built-in loopback test for IC RF transceivers," *IEEE Trans. VLSI Syst.*, vol. 18, no. 6, pp. 933–946, 2010.

[10] J. Dabrowski, "BIST model for IC RF-transceiver front-end," in *Proc. IEEE Defect and Fault Tolerance in VLSI Systems (DFT 2003)*, Nov. 2003, pp. 295 – 302.

[11] Y.-P. Lin and P. Vaidyanathan, "Periodically nonuniform sampling of a new class of bandpass signals," in *Proc. IEEE Digital Signal Processing Workshop*, Sep. 1996, pp. 141 –144.

[12] A. Kohlenberg, "Exact interpolation of band limited functions," *J. Appl. Physics*, vol. 24, no. 12, pp. 1432 –1436, Dec. 1953.

[13] B. Razavi, *RF microelectronics*. Prentice Hall PTR, 1998.

[14] P. Cruz and N. B. Carvalho, *Advanced Microwave and Millimeter Wave Technologies Semiconductor Devices Circuits and Systems*. Austria: In-Tech, 2010, ch. 25 - Receiver Front-End Architectures - Analysis and Evaluation.

[1 R. Vaughan, N. Scott, and D. White, "The theory of bandpass sampling," *IEEE Trans. Signal Process.*, vol. 39, no. 9, pp. 1973–1984, Sep. 1991.

[ero Ben Kalaia, J.-F. Naviner, and P. Loumeau, "Mixed-signal w calibration technique for time-interleaved adcs," *IEEE Trans. Circuits Syst. I*, vol. 55, no. 11, pp. 3676 –3687, Dec. 2008.

[S. Jamal, D. Fu, M. Singh, P. Hurst, and S. Lewis, "Calibration of time error in a two-channel time-interleaved analog-to-digital conv EEE Trans. Circuits Syst. I*, vol. 51, no. 1, pp. 130 – 139, Jan. 2004.

[V. Arkesteijn, E. A. M. Klumperink, and B. Nauta, "Jitter requirements pling clock in software radio receivers," *IEEE Trans. Circuits Sys* vol. 53, no. 2, pp. 90–94, 2006.

[C. C roy, D. Cline, and P. Gray, "An 8-b 85-ms/s parallel pipeline a/d conv er in 1-micro m CMOS," *IEEE J. Solid-State Circuits*, vol. 28, no pp. 447 –454, Apr. 1993.

[2 u, K. Dyer, S. Lewis, and P. Hurst, "A digital background calibration technique for time-interleaved analog-to-digital converters," *IEEE J. Solid-State Circuits*, vol. 33, no. 12, pp. 1904 –1911, Dec. 1998.

[21] Y. Jeng, "Digital spectra of non-uniformly sampled signals: theories and applications. i. fundamentals and high speed waveform digitizers," in *Proc. IEEE Instrum. and Meas. Technol. Conf. (IMTC-88)*, Apr. 1988, pp. 391 –398.

[22] P.-I. Mak, S.-P. U, and R. Martins, "Transceiver architecture selection: Review, state-of-the-art survey and case study," *IEEE Circuits Syst. Mag.*, vol. 7, no. 2, pp. 6–25, 2007.

[23] J. Chen, "Modeling RF systems," The Designer's Guide Community, 2005. [Online]. Available: http://www.designers-guide.org/Modeling/modeling-rf-systems.pdf